Pergamon

Solid State Communications, Vol. 100, No. 1, pp. 47–51, 1996
Published by Elsevier Science Ltd

0038–1098/96 $12.00+.00

PII: S0038-1098(96)00375-4

ORIENTATIONAL SUPERLATTICES IN ORDERED $GaInP_2$

A. Mascarenhas, Yong Zhang, R. Alonso and Sverre Froyen

National Renewable Energy Laboratory, Golden, CO 80401, U.S.A.

(*Received* 6 *March* 1996; *accepted* 31 *May* 1996 *by E.E. Mendez*)

Novel results on the electronic properties of superlattices of orientational domain boundaries in ordered $GaInP_2$ are presented. These superlattices exhibit spatially varying amplitudes for their Bloch states, modifications to the band gap, and the appearance of sub-bands and minigaps resulting from periodic perturbations to the angular momentum of electrons. Characteristic features of five distinct polytype structures are discussed in relation to their symmetries. Published by Elsevier Science Ltd

Keywords: A. semiconductors, D. order–disordered effects, D. electronic band structure.

The order–disorder structural phase transformation in several epitaxially grown semiconductor alloys has been shown to generate changes to their optical and electronic properties that may be technologically desirable [1]. In the $GaInP_2$ alloy system, the phase transition from the high symmetry zinc-blende phase ($F\bar{4}3m$) to the low symmetry CuPt phase ($R3m$) that results from spontaneous ordering on the cation sublattice is characterized by an order parameter that varies smoothly as a function of growth parameters [2]. In such a transformation due to an instability at the L points at the Brillouin zone (BZ) boundary, any of the equivalent L points corresponding to the arms k_L^* of the star of the wave vector $\mathbf{k}$ can collapse to the Γ point of the BZ, resulting in the emergence of any of four ordered subvariants. The number of arms in the star equals the index of the subgroup $R3m$, and the subvariants corresponding to the respective arms are the orientational states or ordered domains comprising the low symmetry phase. Since the point groups $3m$ and $\bar{4}3m$ corresponding to the low- and high-symmetry phases, describe different crystal systems, the orientational states can be distinguished by a symmetric second rank tensor, and so the phase transition is ferroelastic [3]. The symmetry breaking across the structural phase transition is associated with the spontaneous emergence of non-zero components of a tensor that is traceless, symmetric, of order two, and serves to distinguish the orientational states. Since the point groups $3m$ and $\bar{4}3m$ are polar and non polar, respectively, the orientational states can also be distinguished by a vector and so the phase transition is also pyroelectric [4]. Owing to the fact that the epitaxial ordering process is driven by surface as opposed to bulk energetics, at most two subvariants have been simultaneously observed to alternate in space [5]. The interface between them is an orientational domain boundary (ODB). The ability to grow samples with one [6] or two subvariants, as well as artificially tailor [7] the period of their alternating sequence has been experimentally demonstrated, making it appealing to investigate the electronic properties of a superlattice of ODBs in an ordered alloy.

In this work we present novel results on the electronic properties of a superlattice (SL) of ODBs in ordered $GaInP_2$. A single period of such a SL consists of two regions, A and B, stacked along the SL axis so that the unit cell in region B can be obtained from that of region A by the action of a rotation operator R that belongs to the point group of the disordered alloy. In such structures, the anion sublattice is unchanged from that of the disordered alloy but the ordering axis for cations is rotated periodically in space. The comprise a subset of a class of superlattices termed orientational superlattices. Some examples of other subsets of this class are the polytypes [8] of SiC and hypothetical periodic arrays of twinned stacking faults [9] in Si. Both are generated by periodic alterations to the hexagonal close-packed stacking sequence (ABCABC...) of atomic planes of the bulk alloy by a rotation R about the stacking axis that does not

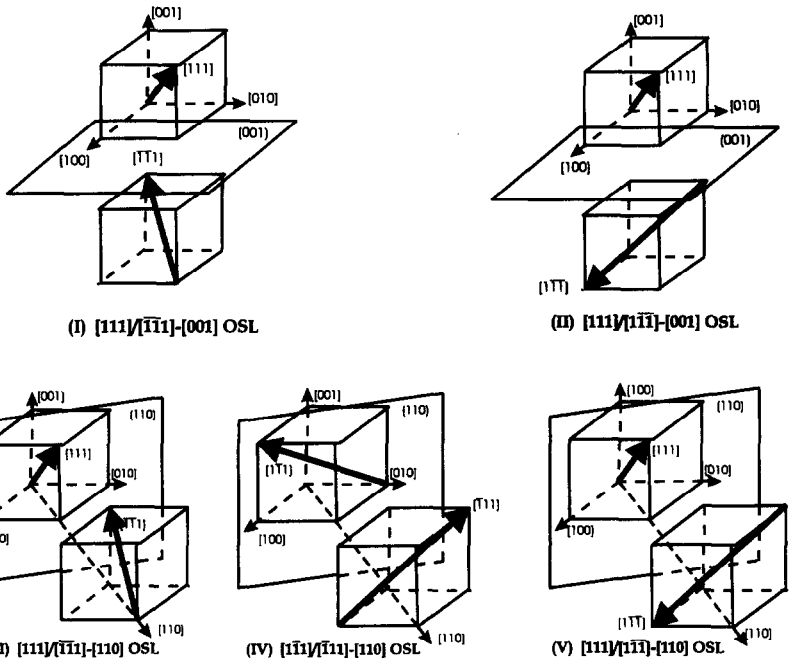

Fig. 1. Five polytype orientational superlattices based on CuPt-ordered $GaInP_2$ alloys. The arrows denote the pyroelectric vector generated in the zinc-blende unit cells of the ordered subvariants on either side of an ODB interface as a result of ordering.

belong to the point group of the parent alloy. In contrast, the ODB superlattices in $GaInP_2$, which consist of a periodic stacking sequence of ordered subvariants, are zero defect superlattices to the order of perturbations to the parent alloy ($F\bar{4}3m$) but exhibit ODB defects in the $R3m$ symmetry of the ordered alloy. We now show that these superlattices exhibit modifications to the valence bands and wave functions of the ordered alloy even in the absence of band edge and effective mass discontinuities, and that these result from periodic perturbations to the angular momentum of the electrons.

If atomic arrangements at the substrate interface are neglected, there are five distinct ODB structures (polytypes) that are possible, as shown in Fig. 1. The arrows denote the direction of the pyroelectric [4] vector. The reversal in the direction of any one of the arrows depicted for the polytypes in Fig. 1 is associated with the additional occurrence of a zinc-blende antiphase boundary at the same interface as the ODB. This antiphase boundary is generated by combining the rotation R of the unit cell of region A with a translation T' that does not belong to the space group $F\bar{4}3m$ (it interchanges cation planes with anion planes). Translations T that interchange the Ga and In cation planes belong to $F\bar{4}3m$ but not to $R3m$ and do not reverse the direction of the pyroelectric vector. ODB structures associated with the additional occurrence of antiphase boundaries generated by T' or T are not considered in this work. Polytype I which consists of a superlattice with [1 1 1] and [$\bar{1}$ $\bar{1}$ 1] subvariants spatially alternating along the [0 0 1] direction has been observed experimentally [5]. Due to the large band gap of $GaInP_2$ ($E_g \gg 2$ eV), the ordering induced change in the coupling of the conduction band to the valence bands (VBs) is weak and is therefore ignored in the following analysis. The SL is denoted by (ABABAB...), where the point groups for regions A and B of the SL differ only by a similarity transformation using the operator R and hence are conjugated in $\bar{4}3m$. The perturbation to the Γ_{15} valence band electronic structure of the alloy due to spontaneous ordering can be modelled [10, 11] using a strain tensor ϵ to emulate the effects of the order parameter θ. The Luttinger Hamiltonian for the CuPt-ordered alloy in region A of the SL can be written as a function of wave vector $\mathbf{k}$ as

$$H_{\mathrm{ord}}(\mathbf{k}) = H_{\mathrm{dis}}(\mathbf{k}) + h(\epsilon), \tag{1}$$

$H_{\mathrm{dis}}(\mathbf{k})$ is the **k.p** Hamiltonian for the disordered alloy using the virtual-crystal approximation. The parameters of $H_{\mathrm{dis}}(\mathbf{k})$ are obtained by averaging those of GaP and InP as detailed in [11]. $H_{\mathrm{dis}}(\mathbf{k})$, when expressed in the subspace $\Gamma_8 \otimes \Gamma_7$ of the irreducible representations of its point group $\bar{4}3m$ that describes its VBs is given by equation (A6) of [11] for a reference frame (x, y, z) oriented along the cubic axes [1 0 0], [0 1 0], and [0 0 1], respectively. Terms due to the lack of inversion symmetry of $\bar{4}3m$ are small and therefore ignored, and so

Table 1. Band-edge energy differences between the top most VB in ordered $GaInP_2$ and the five polytype SLs of $GaInP_2$ with values of the modulation amplitude of the strain ϵ along the SL axis for the polytypes I–V

	I	II	III	IV	V
$E_{SL} - E_{ord}$(meV)	2.46	2.47	3.22	1.71	2.12
$\frac{1}{2}(\lvert\epsilon_A \cdot u\rvert + \lvert\epsilon_B \cdot u\rvert)$	$\sqrt{2}\epsilon$	$\sqrt{2}\epsilon$	$\sqrt{3}\epsilon$	ϵ	$\frac{1}{2}(1+\sqrt{3})\epsilon$

the dipole moment responsible for the pyroelectric effect is neglected. The perturbative Hamiltonian $h(\epsilon)$ due to ordering of the cations is [10–12]

$$h(\epsilon) = -d \sum_{j>1} (L_i L_j + L_j L_i)\epsilon_{ij}, \tag{2}$$

where d is the crystal-field splitting parameter [10, 11], L_i the ith component of angular momentum **L**, and ϵ_{ij} the i,jth component of the strain tensor ϵ_A that emulates the effect of ordering in region A. This term introduces the rhombodhedral distortion of the zinc-blende unit cell due to ordering. The envelope function technique [13] is used to determine the SL eigenstates. Assuming the SL axis is along z' and $z' = 0$ is at the center of region A, the strain tensor is rotated periodically as a function of z', where

$$\epsilon(z') = \epsilon_A + (\epsilon_B - \epsilon_A)\theta(|Z'| - L_A/2), \tag{3}$$

$\theta(|Z'| - L_A/2) = 1$ for z' in region B and $= 0$ elsewhere. $\epsilon_B = R\epsilon_A R^{-1}$ is the strain tensor in region B, where the rotation R belongs to $\bar{4}3m$ but not to the point group $3m$ of the ordered alloy. To the order of perturbations to the zinc-blende lattice, the superlattice potential is

$$\Delta h(z') = [h(\epsilon_B) - h(\epsilon_A)]\theta(|z'| - L_A/2). \tag{4}$$

Regions A and B are assumed to have the same order parameter. The eigenvalue equation for the SL is

$$[H_A\left(q_3 \rightarrow -i\frac{\partial}{\partial z'}\right) + \Delta h(z')]\mathbf{F} = E\mathbf{F}, \tag{5}$$

where $H_A(\mathbf{k}) = H_{dis}(\mathbf{k}) + h(\epsilon_A)$, **F** is an envelope function in the $\Gamma_8 \otimes \Gamma_7$ subspace and if the z' axis differs from [0 0 1], (x,y,z) are transformed to (x',y',z') and $\mathbf{k} = (k_x, k_y, k_z)$ to $\mathbf{q} = (q_1, q_2, q_3)$ with q_3 parallel (//) to z' and q_1, q_2 perpendicular ($\perp$) to z'. A Fourier transform method [14] is used to solve the eigenvalue equation (5). Since regions A and B are oriented symmetrically with respect to the SL axis in polytypes I–IV, not only are there no band offsets but also no effective mass discontinuities for states with wave vectors parallel to the SL axis. However, for polytype-V, there is a discontinuity in the effective mass parallel to the SL axis, and there are no band offsets only at $\mathbf{q} = 0$. Polytypes I–IV are pure orientational superlattices. For the calculations, a value of the strain (in [11] this corresponds to the crystal-field splitting parameter $d = -15$ meV) is chosen so as to obtain typical experimental values $= 25$ meV for the heavy–light hole splitting and $= 90$ meV for the band gap reduction. Table 1 shows band edge energy differences between the top most VB in ordered $GaInP_2$ and the five polytype SLs of $GaInP_2$ for $L_A = L_B = 100$ Å. It is evident that the band gap of the SL structures tends to increase from that of "bulk" ordered $GaInP_2$, an effect similar to the confinement effect that results from band offsets in conventional [15] SL structures. This increase is largest for polytype-III, smallest for polytype-IV, and the same intermediate value in polytypes-I and II. Figure 2 shows the energy dispersion curves for a type-III SL. In addition to the increase in the band gap, sub-bands appear as a result of the folding of the BZ as shown in Fig. 2a. For the asymmetric SL, the lack of symmetry with respect to the rotation R removes the degeneracy at the BZ boundary and mini-gaps appear there as shown in Fig. 2b. Figure 3 shows the probability distribution $P(z')$ for the band edge states. In contrast with bulk semiconductors, even in the absence of energy band discontinuities, the amplitudes of the Bloch states of the SL vary as a function of z'. This amplitude modulation results from interference between Bloch states scattered due to the mismatch of their angular momentum in regions A and B at the ODB interfaces. Figure 4a shows the shift in the VB edge as a function of $L_A + L_B$ for different L_A/L_B ratios. A general feature (typical of type-I–IV SLs) observed is that this energy shift is maximized for a symmetric SL and increases as $L_A + L_B$ is decreased. It is

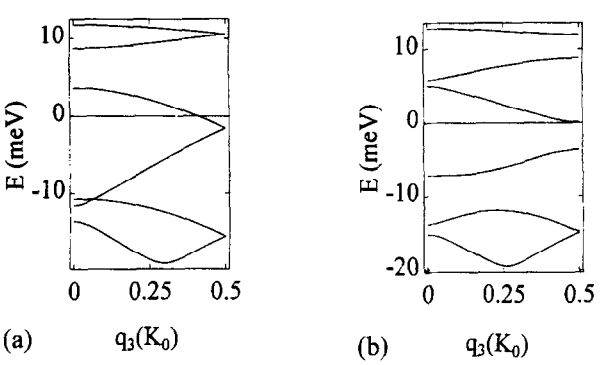

Fig. 2. Energy dispersion curves of the type III SL along the superlattice axis: (a) symmetric, $L_1 = L_2 = 100$ Å; (b) asymmetric, $L_A = 50$ Å and $L_B = 150$ Å. $K_0 = 2\pi/(L_A + L_B)$.

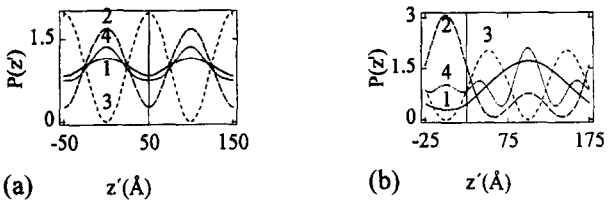

Fig. 3. Probability distributions of the first to fourth valence band-edge states (labelled 1 to 4) for the type III SL: (a) symmetric, $L_A = L_B = 100$ Å; (b) asymmetric, $L_A = 50$ Å and $L_B = 150$ Å.

not possible to obtain bound states in quantum well structures made of polytype I–IV structures for any L_A/L_B ratio.

In a reference frame (x, y, z) with z// [1 1 1] and y// [$\bar{1}$10] the non-zero elements of the strain tensor ϵ_A are $\epsilon_{xx} = \epsilon_{yy} = -\epsilon$ and $\epsilon_{zz} = 2\epsilon$. In this reference frame, the perturbation Hamiltonian for ordering in region A is

$$h(\epsilon_A) = -d\,(3L_z^2 - L^2)\epsilon, \tag{6}$$

where L_z is the z component of angular momentum, and the symmetry modifying term $-3d\epsilon L_z^2$ makes z the preferred or uniaxis in region A. The rotation R, which transforms region A to region B in the SL, changes the strain tensor ϵ_A to $\epsilon_B = R\epsilon_A R^{-1}$ and the perturbative Hamiltonian $h(\epsilon_A)$ to $h(\epsilon_B) = Rh(\epsilon_A)R^{-1}$. In contrast with the band offset perturbations of conventional [13], $h(\epsilon_B)$ is not diagonal in the $\Gamma_8 \otimes \Gamma_7$ subspace and represents the discontinuity in the angular momentum sensed by an electron moving across the ODB interface. Since both ϵ_A and $h(\epsilon_A)$ are traceless symmetric second rank irreducible tensors, the change in $h(\epsilon_A)$ brought about by the rotation R must correlate with the change in ϵ_A brought about by R. If $\mathbf{u}$ is a unit vector // the SL axis, then $\frac{1}{2}(|\epsilon_A\mathbf{u}| + |\epsilon_B\mathbf{u}|)$ represents the modulation amplitude of the strain ϵ along the SL axis. The confinement energies (that result from the probing of the superlattice potential $\Delta h = h(\epsilon_A) - h(\epsilon_B)$ by its wavevector q_3) should correlate with Δh and hence with $\frac{1}{2}(|\epsilon_A\mathbf{u}| + |\epsilon_B\mathbf{u}|)$ which is confirmed in Table 1. The characteristics of the five polytype SLs depend on their symmetries. The axis for the rotation operator R is [0 0 1] for polytypes I, III and IV, and [1 0 0] for polytypes II and V. For polytypes II, III, and IV the SL axis is orthogonal to that of the rotation operator R. The type-III symmetric SL axis is perpendicular to a mirror symmetry plane. In a reference frame with z// [0 0 1], $\mathbf{u}$// [1 1 0] which is the SL axis and the origin located at an ODB interface, its Hamiltonian H commutes with K and Π_u, where K is the time reversal operator, and Π_u is the operator for mirror reflection in a plane $\perp\mathbf{u}$. If $R_z(\pi) = R$ is the operator for rotation about the z axis by an angle π, then $\phi_q(\mathbf{u}) = R_z(-\pi)[K\phi_q(-\mathbf{u})]$ for $\mathbf{q}$// the SL axis, and so

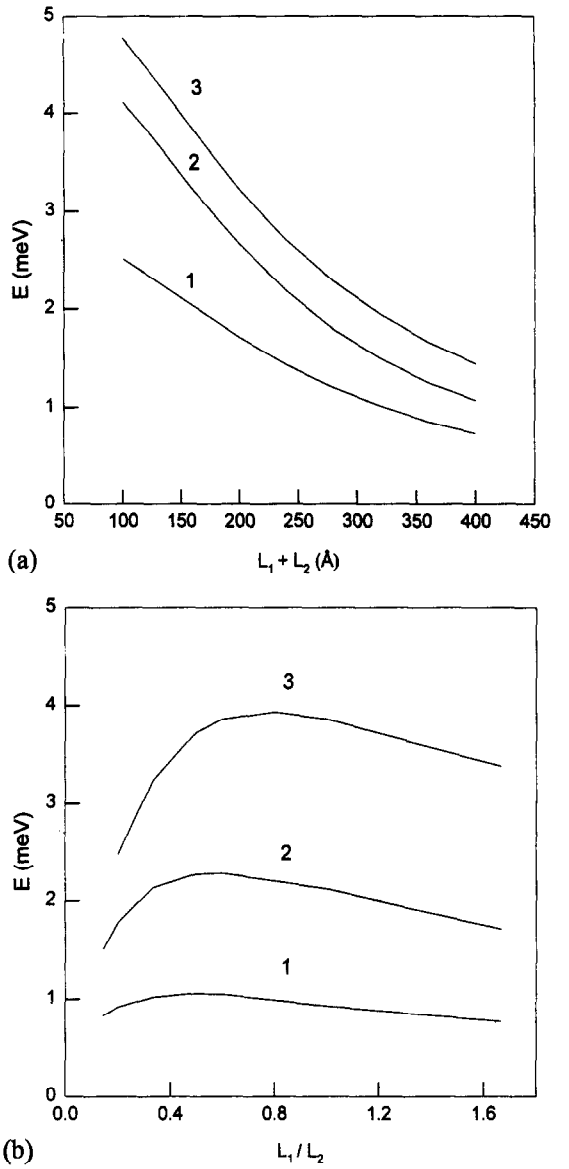

Fig. 4. Confinement energy of the first sub-band as a function of (a) superlattice period $L_A + L_B$ for a type III SL at various L_A/L_B ratios: "1" for 1/5, "2" for 1/2 and "3" for 1/1 (b) L_A/L_B ratio for a type-V SL at various superlattice periods $L_A + L_B$: "1" for 400 Å, "2" for 200 Å and "3" for 100 Å.

the behaviour of an eigenstate of the SL in region B is emulated by the behaviour of the time reversed conjugate eigenstate at the mirror image point in region A rotated by $R_z(-\pi)$. In polytype-I the SL axis is parallel to that of the rotation operator R and so $\mathbf{u}$//z// [0 0 1]. For a symmetric SL of this type, H commutes with the point group element $\{R|\ell\}$, where ℓ is the fractional translation along the z axis for a SL of period 2ℓ and so $\phi_q(u + \ell) = e^{iq\ell}R_z(\pi)\phi_q(u)$ for u located in region A. For polytype-V the SL axis is not orthogonal to that of R. For this polytype only, even for q_1 and $q_2 = 0, H_{ord}$ in region A

differs from $RH_{ord}R^{-1}$ in region B since the effective masses corresponding to the respective orientations of H_{ord} in regions A and B are different. In addition to the pure orientational SL effect there is an effective mass SL effect [16]. In contrast with polytypes I–IV (see Fig. 4a), Fig. 4b shows that the shift in the VB edge maximizes for $L_A/L_B < 1$ where L_A is the region with a larger effective mass along the SL axis. It is possible to obtain bound states in QW structures of polytype V.

To conclude, we have analysed SLs constructed from subvariants of ordered $GaInP_2$ and shown that SL effects on the VB structure result from discontinuities in the angular momentum sensed by the electronic states. They lead to spatially varying amplitudes for the SL Bloch states, modifications to the band gap, and the appearance of minigaps. The shift in the valence band energy calculated in Table 1 for structures with order parameters [11] close to 0.5 and SL periods of 200 Å are small but increase to values as high as 16 meV for order parameters close to unity and SLs with a period of 40 Å. Although only SLs constructed from subvariants of the star of the wavevector **k** generated in the $F\bar{4}3m$ to $R3m$ structural phase transition have been studied in this article, the analysis provided is sufficiently general to be applied to similar disorder–order transitions in other alloys. The energy shifts will be higher for alloys with larger crystal field splittings.

Acknowledgement—This work was supported by the Office of Energy Research Material Science Division of the DOE under contract No. DE-AC36-83CH10093.

REFERENCES

1. Zunger, A. and Mahajan, S., *Handbook of Semiconductors*, Vol. 5 (Edited by T.S. Moss), p. 1399. Elsievier, Amsterdam, 1994.
2. Alonso, R.G., Mascarenhas, A., Horner, G.S., Bertness, K.A., Kurtz, S.R. and Olson, J.M., *Phys. Rev.* **B48,** 1993, 11833.
3. Aizu, K., *J. Phys. Soc. Jpn.* **27,** 1969, 387; **34,** 1973, 121.
4. Alonso, R.G., Mascarenhas, A., Horner, G.S., Sinha, K., Zhu, J., Friedman, D.J., Bertness, K.A. and Olson, J.M., *Solid State Commun.* **88,** 1993, 341.
5. Morita, E., Ikeda, M., Kumagai, O. and Kaneko, K., *Appl. Phys. Lett.* **53,** 1988, 2164.
6. Horner, G.S., Mascarenhas, A., Alonso, R.G., Friedman, D.J., Sinha, K., Bertness, K. and Olson, J.M., *Phys. Rev. B, Rapid Commun.* **48,** 1993, 4944.
7. Chen, G.S. and Stringfellow, G.B., *Appl. Phys. Lett.* **59,** 1991, 324.
8. Backes, W.H. Bobbert, P.A. and van Haeringen, W., *Phys. Rev.* **B49,** 1994, 7564.
9. Ikonic, Z., Srivastava, G.P. and Inkson, C.J., *Phys. Rev.* **B48,** 1993, 17181.
10. Wei, Su-Huai and Zunger, A., *Appl. Phys. Lett.* **64,** 1994, 757.
11. Zhang, Yong and Mascarenhas, A., *Phys. Rev.* **B51,** 1995, 13162.
12. Bir, G.L. and Pikus, G.E., *Symmetry and Strain-Induced Effects in Semiconductors*. Wiley, New York (1974).
13. Bastard, G., *Wave Mechanics Applied to Semiconductor Heterostructures.* Les Editions de Physique, Les Ulis Cedex, 1988.
14. Baraff, G.A. and Gershoni, D., *Phys. Rev.* **B43,** 1991, 4011.
15. Esaki, L. and Tsu, R., *IBM J. Res. Dev.* **14,** 1970, 61.
16. Sasaki, Akio., *Phys. Rev.* **B30,** 1984, 7016.